Ageing of Alkylthiol-Stabilized Gold Nanoparticles

Johann Lacava, Anika Weber, and Tobias Kraus

Ageing of alkylthiol-stabilized gold nanoparticles

Johann Lacava, Anika Weber, and Tobias Kraus[*]

Structure Formation Group,

INM — Leibniz Institute for New Materials,

Campus D2 2, 66123 Saarbrücken, Germany

E-mail: tobias.kraus@inm-gmbh.de

Phone: +49-681-9300-359. Fax: +49-681-9300-279

Abstract

The ageing of spherical gold nanoparticles having 6-nanometer-diameter cores and a ligand shell of dodecanethiol was investigated under different storage conditions. We quantified losses caused by agglomeration and changes in optical particle properties. Changes in colloidal stability were probed by analytical centrifugation in a polar solvent mixture. Chemical changes were detected by elementary analysis of particles and solvent. Fractionation occurred under all storage conditions. Ageing was not uniform but broadened the property distributions of the particles. Small-number statistics in the ligand shell density and the morphological heterogeneity of particles are possible explanations. Washing steps exacerbated ageing, a process that could not be fully reversed by excess ligands. Dry storage was not preferable to storage in solvent. Storage under inert argon atmosphere reduced losses more than all other conditions but could not prevent it entirely.

[*]To whom correspondence should be addressed

Introduction

Gold nanoparticles (AuNP) are ancient pigments, modern indicators in biochemical assays, and important model particles for colloidal science. Excellent control over size, size distribution and shape and the ease of surface modification via thiol chemistry have made them popular in applications and fundamental studies alike. Understanding their behaviour is the basis for their industrial use and the interpretation of colloidal experiments on them.

Ligand molecules on the AuNP surfaces control the growth of the particles during synthesis and prevent particle aggregation. Typical ligands have functional groups that bind covalently to the gold surface. It is tempting to imagine such layers as a solid "shell" that protects the gold core and imparts it with solubility in liquids that interact with the ω-functionality of the ligand. In reality, even the comparatively strong bonds between thiol-bearing ligands and the nanoparticle surface undergo dynamic binding and unbinding processes.[1–3] The ligand shell is a complex and dynamic entity. It can age and change its properties with time.

This is not unique to AuNPs. Anecdotal evidence suggests that ageing occurs (depending on storage conditions) for many technically relevant nanoparticles: it is a common advise to use freshly synthesized particles for material synthesis or studies on colloidal stability. We are not aware of a systematic study on the storage stability of different nanoparticles. The following briefly summarizes publications on different particle types that observed ageing.

Dollefeld et al. explained the apparent shrinkage of thiol-capped cadmium chalcogenide nanoparticles detected by analytical ultracentrifugation and optical spectroscopy by ligand desorption.[4] They used NMR to show the constant dynamic replacement of ligand molecules and argued that losses are to be expected in the absence of excess free ligand. Kalyuzhny and Murray reported ligand losses during the purification of CdSe nanocrystals.[5] The degradation on thiol-stabilized CdSe nanocrystals in water[6] and the

oxidation of dry Co nanocrystals in air[7] have also been observed.

Ligand layers are often imagined as a uniform organic shells wrapped around spherical metal cores. On planar gold surfaces, many thiols form self-assembled monolayers (SAMs) with ordered and uniform geometries. On AuNPs, the ligands encounter not only different crystal facets, but also a multitude of edges, terraces and vertices, resulting in binding sites with different affinities for the ligand molecules.[8,9] The resulting layers have complex structures that depend on the exact core geometry. Ligand-solvent interactions vary over the particles' surfaces, which affects colloidal stability. Reorganization of the ligand layers can occur as a result of the dynamic equilibrium between free and surface-bound ligand molecules or involve practically irreversible chemical reactions, such as oxidation of ligands or surface sites. It can be a slow process that causes gradual changes in particle behaviour.

Dasog and Scott reported on the stability of thiol-coated gold particles that they synthesized using a modified Brust-Schiffrin protocol.[10] Oxidation of the anchored thiol groups lead to Ostwald ripening and precipitation of the particles. Halide anions were necessary for this reaction to occur in air.

Chechik and others studied reaction rates of place-exchange reactions between n-butanethiol-protected AuNP and disulfides using electron spin resonance.[11,12] They observed that aged samples showed decreasing exchange rates and attributed the decrease in the number of defect sites as the original ligand slowly reorganized. The reorganized ligands on aged nanoparticles exhibited higher desorption temperatures in thermogravimetry: a case where ageing improved the stability of the particles.

Ligand surface density is known to affect the properties of nanoparticles. For example, poly(ethylene glycol)s (PEGs) — widely used as as ligands for nanoparticles in biology and medicine — lend nanoparticle non-fouling properties depending on their density.[13] At low PEG density, the units on a surface are organized in a so-called mushroom configuration, whereas at higher PEG density they display a brush configuration.[14] Only the

brush configuration provides an optimal surface protection against opsonization. It is unclear whether and how the surface density of the PEG changes as such particles age under different conditions.

In this contribution, we discuss the ageing of a simple particle system, AuNPs with dodecanethiol ligands stored in unpolar solvent. We studied changes in optical properties, colloidal stability, and the resulting loss after storage. Particle handling was choreographed to mimic typically employed protocols (filtering, ultrasonication, etc.), standardized for a systematic study. Storage at different temperatures, with different headspaces, and after different purification protocols was compared.

Experimental section

The choice of storage conditions was based on a literature review. Most nanoparticle dispersions are stored at room temperature[4,7,15] or at lower temperature.[16] Sometimes, excess ligand was added to the suspension to ensure optimal surface coverage especially for ligand-exchange reaction.[17,18] In some cases, the suspension was stored under Argon.[16,19]

A single particle batch was used for each storage condition to avoid batch-to-batch variations. The timing of all handling steps was identical within the errors of manual handling.

Gold nanoparticle synthesis

Gold nanoparticles with core diameters of 6 nm were synthesized using a route adapted from Zheng et al.[20] They were formed in a one-pot reduction of a gold source by an amine-borane complex in the presence of an alkylthiol. Chlorotriphenylphosphine gold (ABCR, minimum purity 98%) was mixed with dodecanethiol (DT) (Fluka, 98%) in benzene (Riedel-de-Hahn, 99.5%) to form a clear solution to which tert-butylamine-borane

complex (Fluka, 97%) was subsequently added. The mixture was heated to 55 °C for 1 h during which the solution turned into a dark purple colour indicating nanoparticle formation. After the reduction reaction the gold nanoparticle dispersion was cooled to room temperature (RT), the particles were precipitated by the addition of ethanol, washed by centrifugation and subsequently resuspended in hexane (samples (a),(b) (c) (e) (f) and (g)) or toluene (sample (d)). A batch of 40 mL was produced and divided into 4 aliquots (samples (a),(b) (c) and (d) or samples (a),(b) (e) and (f) or 2 samples (a) and 2 samples (g)). The concentration of gold in hexane for all batches was 3.6 mg/mL, corresponding to approximately 1.3×10^{15} particles/cm^3.

Sample storage

After synthesis, samples were prepared and stored under different conditions:

- Sample (a) was stored at 23 °C on the lab bench and wrapped in aluminium foil to exclude light.

- Sample (b) was stored at 7 °C in the fridge.

- Sample (c) was aliquoted in 5 vials of 2 mL. All aliquots were dried in vacuum at room temperature. The dry particles were stored at 23 °C, wrapped in aluminium foil to exclude light.

- Sample (d) was resuspended in toluene. The particles were precipitated by the addition of the same volume of ethanol, washed 5 times by centrifugation and subsequently resuspended in hexane. The sample was then stored at 7 °C in a refrigerator.

- Sample (e) was stored at 23 °C and wrapped in aluminium foil to exclude light. A fraction of 0.0125% per volume of dodecanthiol was added, the resulting dispersion was vortexed for 1 min, precipitated by the addition of the same volume of ethanol, washed by centrifugation, and finally resuspended in hexane.

- Sample (f) was treated exactly as sample (e), but with a fraction of 0.125% per volume of dodecanethiol.

- Sample (g) was stored at 23 °C under argon atmosphere, wrapped in aluminium foil to exclude light.

Characterization

Dynamic light scattering, UV-Vis spectroscopy and analytical centrifugation were performed on all samples every week. Details on the preparation of the sample are given in the Supporting Information. Atomic absorption spectrometry (AAS) was used for the determination of gold content for samples (a), (b), (e) (f) and (g) every week.

Dynamic Light Scattering

Particle sizes were characterized via Dynamic Light Scattering (DLS) to measure the hydrodynamic radius of the primary particles and determine whether agglomeration occurred. We used a Wyatt Technology Dyna Pro Titan operating at a laser wavelength of 831.2 nm. Filtered samples were diluted 100 times and measured at a scattering angle of 90°. The relaxation time distribution was recovered using the CONTIN analysis of the autocorrelation function and converted to hydrodynamic particle radii using solvent viscosity values from literature.

UV-Vis spectroscopy

Particle concentrations were determined by UV-Vis spectroscopy to calculate the fraction lost through sedimentation and filtration. Transmission UV-Vis spectra were recorded on a Cary 5000 photospectrometer (Varian Inc., USA) in the wavelength range from 200 nm to 800 nm.

Dilution was necessary to operate in the optimal dynamic range of the instrument.

For each sample, we chose a dilution ratio d_{uv} based on the maximum absorbance of fresh (non-aged) dispersions such that $A_{w1}(\lambda \approx 517\text{nm}) = 0.65 \pm 0.03$. This dilution was then used for all measurements on the sample while it aged. For each time step, approximately 1 mL of each diluted sample was characterized in quartz cuvettes having a beam path of 1 cm. A hexane spectrum was subtracted from the samples' spectra as background.

Spectra were obtained both for both filtered and unfiltered samples to calculate the particle loss in filtration.

Atomic absorption spectrometry

The gold content in the solvent was characterized by elementary analysis after all AuNP had been removed. Dispersions were precipitated with the same volume of ethanol and centrifuged at 20500 rpm during 15 min. Gold in the supernatant was quantified using a contrAA 700 high-resolution continuum source atomic absorption spectrometer (HRCS-AAS). The spectrometer was equipped with a xenon short arc lamp as a light source shining through the sample-containing graphite furnace.

A solution of 400 µg/L of gold equivalent in 1-propanol (in the form of chlorotriphenylphosphine gold) was used as standard solution. The samples were diluted with 1-propanol at a volume ratio of 1:10. A volume of 20 µL of the diluted sample was injected into the graphite tube.

Drying, pyrolysis, and atomization in the graphite furnace were performed according to Table 1 in the Supporting Information. Averages of two absorbance values from sequential injections were used throughout the study.

Analytical centrifugation

The polarity of the ageing dispersions was characterized by precipitating them in a polar solvent mixture under analytical centrifugation. Filtered dispersions were mixed with equal volumes of 1-propanol and immediately transferred to cuvettes in a LUMiSizer

multisample analytical centrifuge (L. U. M. GmbH, Berlin, Germany). 1-propanol was chosen as it mixes well with hexane. The centrifuge uses a line array detector and LED light source to measure space- and time-resolved extinction profiles while the sample rotates at defined speed and temperature. Intensities of the transmitted light as a function of time and position over the entire length of the cuvette were recorded (see Supporting Information). Agglomeration and phase separation of the individual samples were compared and analysed by tracing the sedimentation of the particles and their agglomerates.

All measurements were made in polycarbonate tubes (model "synthetic rectangular cell PC", 2 mm transmission path, 0.4 ml filling capacity, L. U. M. GmbH, Berlin, Germany) at velocities from 300 to 2500 rpm. SEPView software provided by the manufacturer was used to control the instrument and analyse data. The evolution of the transmission profiles contains information on particle size distribution and agglomeration kinetics.

Results and discussion

Nanoparticle handling typically involves transfer, sonication, filtration and centrifugation steps. We performed these steps for each stored sample every week and used UV-Vis spectroscopy at the surface plasmon resonance (SPR) together with AAS to quantify losses that occurred during every step. The results provide a rough but useful estimate of losses one can expect for different storage conditions.

More subtle are changes in particle behaviour that do not directly lead to losses but affect functional aspects of the particles. We quantified such changes by analysing the agglomeration state by dynamic light scattering (DLS), the SPR position, and the agglomeration behaviour in polar solvents using analytical centrifugation. Together (and comparing filtered and unfiltered samples) these methods are sensitive to a variety of changes in particle properties that matter when they are used as markers or as components in a

composite material.

An unexpected outcome of the measurements was the fractionation of particles. We consistently found — in ratios depending on storage conditions — a fraction of particles that agglomerated irreversibly and sedimented, a fraction that remained suspended but formed smaller agglomerates, a fraction that remained dispersed but changed its agglomeration behaviour in polar solvents, and a fraction that appeared largely unchanged.

Fractionation can result from imperfect mixing in the storage vessel, when different regions age differently. Alternatively, morphologically different particles in the fresh dispersion may age differently and form the final fractions.

Fractionation can also result from simple statistics. Nanoparticles carry comparatively small numbers of ligand molecules. If the probability for one ligand molecule to desorb during a given time is constant, a broad distribution of ligands-per-particle will form. Particles that loose many ligands will behave differently from particles that retain most ligands. In effect, the homogeneous dispersion splits into different fractions.

From a pragmatic standpoint, it is often interesting under which conditions the fraction of apparently unchanged particles is greatest. In our study, storage under Argon at room temperature was preferable to all other methods in this regard. Even under the best possible conditions, however, fractionation occurred to a non-negligible degree. We discuss it in detail in the next section.

Fractionation by ageing

Dispersions were stored for at least 21 days under different conditions (see section Sample storage) and analysed weekly. Samples were taken from the dispersions following a protocol designed to reflect typical colloid handling methods as applied in practice. Ageing caused fractionation under all storage conditions. The size of the different fractions depended strongly on the storage conditions. After 14 days, all stored samples were unstable in the sense that the freshly filtrated dispersion exhibited increasing particle sizes

in DLS after less then one hour (see Supporting Information).

We analyzed the following fractions every week:

- particles agglomerating in the storage vessel that formed a sediment (fraction 1),

- particles agglomerating in the storage vessel that remained in the filter (fraction 2),

- particles dispersed in the storage vessel that remained dispersed upon adding 1-propanol (fraction 3),

- particles dispersed in the storage vessel that precipitated upon adding 1-propanol (fraction 4).

Fraction 4 dominated freshly prepared dispersions (typically comprising around 60 %). Upon ageing, the first three fractions grew in size for all storage conditions.

Optical spectroscopy was used to quantify the size of fraction 1, fraction 2 and the combined fractions 3 and 4 (the filtered sample). We assumed the absorbance A to be directly proportional to the concentration c for each fraction at the peak wavelength λ_{max}:

$$A = a \times l \times c \tag{1}$$

where a is the absorptivity (dependent on the fraction) and l is the path length of the absorbing medium (only hexane was used for optical measurements).

Mass balances were used to calculate the fractions where necessary: for example, we measured concentrations of freshly prepared, aged but unfiltered dispersions and compared it to the concentration in the filtered dispersions to calculate the amount of particles lost in the filter (fraction 2). Fractions 3 and 4 were quantified using time-dependent optical spectrometry in an analytical centrifuge.

Many standard procedures in dispersion handling are difficult to perform without variation. Filtration results will depend on the exact agglomeration state and tend to remove dispersed particles when many agglomerates are caught in the filter. Representative

sampling from a larger volume is hard when agglomerates are present. When using large volumes, mixing becomes hard. When using small volumes, rapid evaporation distorts concentrations. Random errors on the order of 10% are expected. We report the results of multiple repetitions to give an impression of the variations.

Figure 1 shows the fractionation of samples stored under different conditions at different times. In the following, we discuss which mechanisms are consistent with the observed evolution.
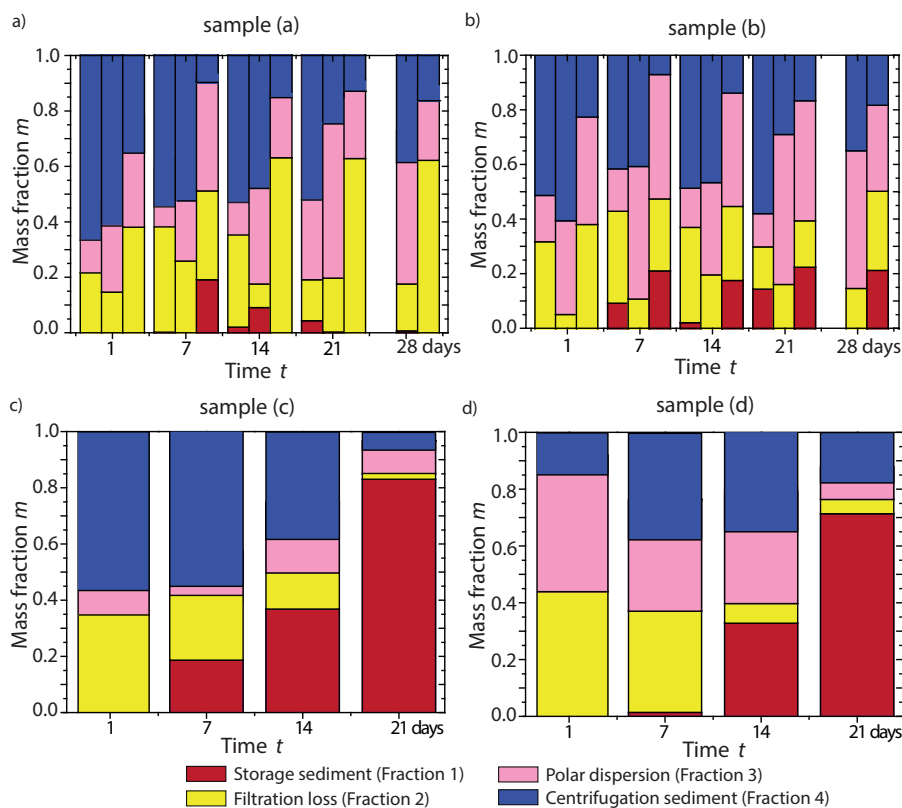
Figure 1: Fractionation of sample (a) sample (b), sample (c), sample (d) by mass as a function of time. For all storage condition, fraction 4 — particles dispersed in the storage vessel that precipitated upon adding propanol — dominated first and shrank with time.

Fraction 1 Losses due to sedimentation in the vessel — did not exceed 20% for the dispersions (a) and (b) stored in liquid without additional treatment. It was greater both for samples stored in dry (c) and washed additionally (d). Redispersion and washing apparently fostered sedimentation.

Fraction 2 Losses in filtration — remained approximately constant for wet storage and shrinks for both dry and washed storage. Particles seemed to move from fraction 2 to 1.

Fraction 3 Dispersed particles stable upon addition of 1-propanol — grew in almost all cases when considering the total amount of particles that remained dispersed.

Fraction 4 Dispersed particles precipitating upon addition of 1-propanol — dominated originally and systematically shrank, usually both overall and compared to fraction 3. Particles appeared to leave this fraction when ageing.

We suggest that fractions 1 and 2 formed through agglomeration. Only agglomerates could sediment on our time scales: fully dispersed particles are Brownian. Filtration may have removed some fully dispersed particles, but only when considerable amounts of agglomerates blocked the filter. Agglomerate sizes controlled whether they sedimented and entered fraction 1 or remained in the liquid and were filtered.

The existence of fractions 1 and 2 directly after synthesis suggest that agglomeration was ubiquitous. Even when using a well-developed, optimized synthetic protocol as we did here, a certain fraction of particles is prone to agglomeration. Most published work uses filtration or centrifugation before using particles to remove the unavoidable agglomerates.[21–24] We believe that nanoparticles from most syntheses involve at least some agglomeration even under optimal conditions.

Agglomeration aggravated during storage. Samples stored under different conditions widely varied in the evolution of fractions 1 and 2 over time. Particles did not agglomerate at a constant rate; depending on storage conditions, agglomeration rates increased. We suggest that inherent properties of particles change during storage.

This hypothesis is further supported by the evolution of fractions 3 and 4. A complex property of particles — their stability in a more polar solvent mixture — was probed to define these fractions. Only particles that did not agglomerate were tested. That the size of fraction 3 changed during storage can only be explained by a change in the particles'

structure. That fraction 3 *increased* upon ageing is surprising.

Fractions 3 and 4 were quantified with an analytical centrifuge as described in the experimental section and in the Supporting Information.

Note that fractionation does not imply sharp transitions in particle properties. It is more likely that certain inherent particle properties change in a continuous fashion. Experiments like precipitation in a polar solvent create fractions containing particles from a range of values of this property (say, particle-solvent interaction). Kinetic effects will likely cause overlaps so that particles having identical properties may end up in different fractions. It is also important to note that in samples where fractions 1 or 2 are dominating, fractions 3 and 4 become small and their analysis is burdened by large statistical uncertainties. We do not report results for samples (c) and (d) due to these uncertainties.
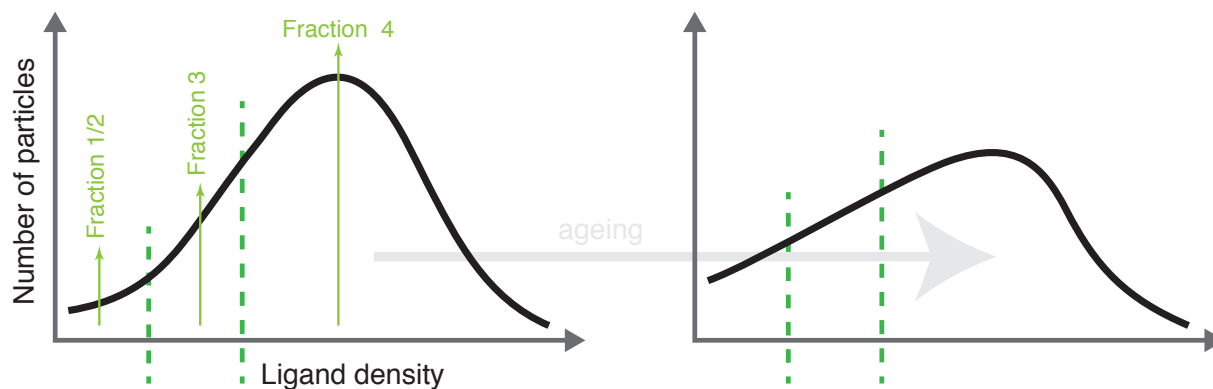
Figure 2: A a schematic model for ageing by ligand desorption.

Let us assume that ageing is caused mainly by a decreasing ligand density (Figure 2). Let us also assume that particles with dense ligand layers are stable against agglomeration in unpolar solvents but rapidly precipitate in more polar solvents. Particles with moderately dense layers slowly agglomerate in unpolar solvents, but remain stable in polar solvents for some time. Particles with sparse layers rapidly agglomerate in unpolar solvents.

All storage conditions lead to a decrease of centrifugation sediment and filtration losses (fractions 1 and 2). Above model explains this effect: in the original population,

the majority of particles had a dense ligand layer. It took a while until this part of the population had lost enough ligands to enter fractions 1 and 2 (Figure 2). Before it did so, more and more particles went through a period with an intermediately dense ligand layer. They caused the increasingly large fraction 3 that is only finally diminished when the majority of particles became unstable.

It is unclear why storage at room temperature (sample (a)) was preferable to fridge storage (sample (b)). Possible explanation include the condensation of water into the solvent (with water increasing the desorption reaction[25]) and temperature-induced agglomeration of particles due to reduced solubility,[26] an effect that could be exacerbated by reduced ligand density.

Drying and redispersion (sample (c)) and extensive washing (sample (d)) both caused immediate ligand loss. In our model, the overall particle population was shifted in ligand density (Figure 2). Many particles entered fractions 1-3 before the storage period started. Further ageing proceeded as expected: intermediately dense ligand layers became sparse, particles were lost in fractions 1 and 2. The amount of particles towards the end of the experiment was so small that statistical fluctuations dominated.

Drying and redispersion (sample (c)) also markedly increased fraction 2, indicating that dry particles could not be redispersed at all. We do now know whether this is due to ligand losses that made them insoluble or due to other morphological changes of the particles in dry state. The results clearly show that simple drying is not a viable option for particle storage. Careful lyophilizing may be less lossy.

The desorption of ligands can explain the fractionation that we observe. We cannot exclude similar, more complicated effects, however: for example, ligand double layers may have been present on some particles. (We analyzed all TEM micrographs of particles for increased spacing expected for such double layers and did not find any, but they may be lost in TEM preparation.) We cannot decide whether the change in particle behaviour was thermodynamic and would occur regardless of the experimental time scales or whether

agglomeration merely become more rapid (or less rapid, in the case of polar solvents) for aged particles.

Evolution of Surface Plasmon Resonance upon ageing

We can excluded fundamentally different mechanisms of ageing (e.g., Ostwald ripening and aggregation) by analysing the surface plasmon resonance (SPR) of the dispersions.

Consider the SPR model derived by Mulvaney based on the Drude approximation:[27]

$$\lambda_{spr} = \lambda_p^2(\epsilon^{NP} + 2\epsilon_m) \tag{2}$$

where ϵ_m is the dielectric constant of the medium, ϵ^{NP} is the dielectric constant of the metallic nanoparticle, and λ_p is the bulk plasmon wavelength:

$$\lambda_p^2 = (2\pi c)^2 \times \frac{m_e \epsilon_0}{N e^2} \tag{3}$$

expressed in terms of the concentration of free electrons N in the metal, the effective mass of electrons m_e, the vacuum permittivity ϵ_0, and the velocity of light c.

A blue shift of the SPR is expected upon a decrease in the medium's refractive index or a change in free electron density of the gold nanoparticles.[28] The former is likely to occur when ligands dissociate. For example, Jain et al. report a gradual blue-shift in the SPR of gold nanoparticles from 525 to 519 nm when irradiating gold nanoparticles carrying thiolated DNA and attributed the shift to the dissociation of the ligand.[29]

A red shift in the SPR can be caused by nearby particles that affect the medium's refractive index. In close proximity, surface plasmons of multiple particle are coupled, and Mulvaney's approximation eventually breaks down.[30–35]

If both agglomeration and ligand desorption occur in storage, one would expect shifts in both directions depending on the storage time, and broadening of the SPR from the

superposition of both effects in different fractions.
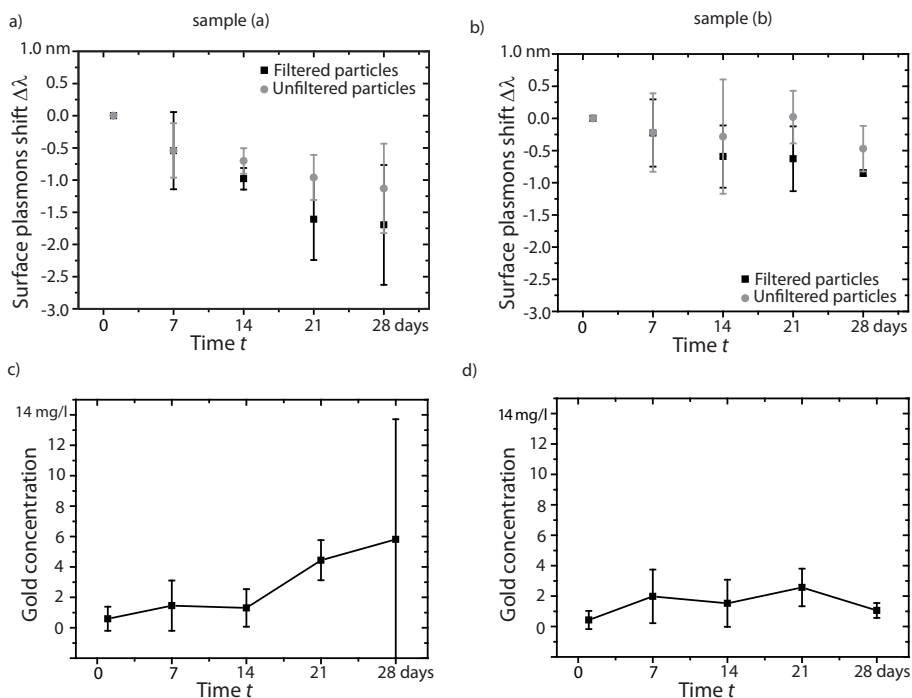
Figure 3: Shifts of the surface plasmon resonance positions during storage in filtered (black) and unfiltered solution (grey) for (a) sample stored at RT and (b) sample stored at 7 °C. Gold concentrations in the supernatants were measured by ICM-OES for (c) sample stored at RT (c) and (d) for sample stored at 7 °C.

Figure 3 a) and b) show the shifts of the SPR from that of the freshly prepared and purified dispersion $\Delta\lambda$ to that of samples stored at RT (sample (a)) and at 7 °C (sample (b)) as a function of time. Blue shifts occurred under both storage conditions, but the shifts at 7 °C were too small to be statistically significant. The width of the SPR peak increased under both storage conditions. The shifts were always greater for filtered than for unfiltered particles, but we did not observe red shifts even in cases where a large fraction of particles had agglomerated.

The observed shifts can only be explained by a change in the refractive index of the particles' dielectric environments. It is hard to imagine any origin other than the desorption of ligand molecules. Our analysis of the spectra is simple and will not separate the SPR spectra of agglomerated and dispersed particles. But it is robust and would detect red shifts caused by agglomeration. The fact that all shifts were towards the blue strongly

suggests that ligand desorption is strong and ubiquitous.

Figure 3 c) and d) show the gold contents of the supernatant after particles had been removed by precipitation with ethanol, centrifugation, and filtration. We found gold concentrations in the solvent that are easily detected by AAS and that would cause a visible colouration if it was due to residual gold particles. Since there was no SPR signature detectable even in the samples with the highest gold content, we conclude that ligand desorption also entails gold desorption. It is unclear in which form gold is removed from the particles; thiolates or very small clusters are possible candidates. Schmid found that even metal clusters made of $Au_{55}(PPh_3)_{12}C_{l6}$ show features in the 520 nm plasma resonance band.[36]

Effects of excess thiol

Ligand desorption during washing may be ameliorated by excess thiol in the solvent. To test this hypothesis, we added the equivalent to 4 mol% (sample (e)) and 40 mol% (sample (f)) of dodecanthiol to freshly prepared dispersions after washing and removed it after a constant time. All other handling was unchanged.

The size of the two samples were analysed using DLS. After 14 days, the two samples were unstable and exhibit increasing particle sizes in DLS after less then one hour (see supporting information).

Figure 4 shows the results obtained for the two samples.

Thiol addition after washing seems to partially revert degradation. The reduced loss in storage sediment, in particular for the smaller thiol addition, supports the idea that washing leads to an immediate loss of ligand that decreases particle stability from the first day. The large fraction of more polar particles may be explained by the thiol acting as a surfactant molecule that forms double layers around the nanoparticles, but it is unclear why a larger thiol concentration should reduce the polar fraction and not sedimentation. The blue shifts in the SPR are somewhat less pronounces than in the absence of thiol, and
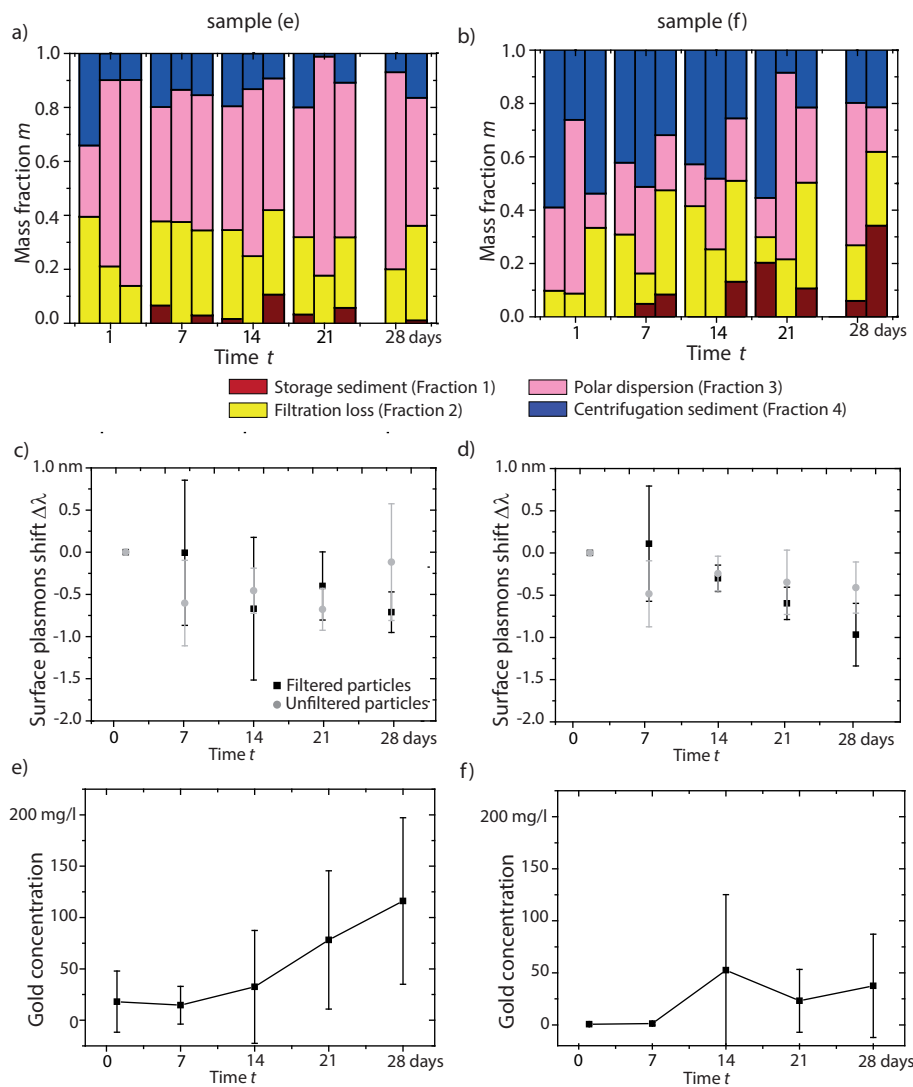
Figure 4: Fractionation of samples treated with (a) 4 mol% (sample (e)) and (b) 40 mol% (sample (f)) dodecanethiol after washing. Surface plasmon resonance shifts (c) and (d) of filtered (black) and unfiltered samples (grey). Gold concentrations (e) and (f) in the supernatant.

we did not observe any red shifts.

Effects of an inert head space

Some authors suggest oxidation as a mechanism leading to ligand loss. For example, films of gold nanoparticles (4 nm diameter) interlinked with 1,9-nanonedithiol and 1,16-hexadecanedithiol were oxidized when stored under ambient condition but remained stable under argon.[37] Oxidation of the thiol groups was observed after two weeks in ambient conditions in the presence of halide anions.[10]

We stored sample (g) under argon at RT and studied it using above routines. Figure 5 (a) shows the evolution of this sample.

The inert atmosphere affected ageing notably. Sedimentation was reduced from the onset and the fraction of polar particles remained small. Samples stored under argon were the only case where we observed red shifts in the SPR spectra, indicating reduced ligand desorption. (The fact that red shifts were only observed in unfiltered samples is consistent with agglomeration shifting the SPR towards red). The magnitude of these changes is surprising, because we did not exclude air or water during synthesis or purification and expect both to be dissolved in the dispersion at the beginning of the storage period.

Summary and conclusions

Alkylthiol-stabilized gold nanoparticles age under commonly used storage conditions. After 2 weeks, more than half of the particles had changed their behaviour when storing them in air at room temperature. Particularly problematic is the fractionation of the homogeneous dispersion into a mixture particles with diverging polarity. Experiments that are affected by particle-solvent interactions will produce subtly misleading results when performed on particles having widely different properties.

The results suggest that ligand loss is a major process responsible for sedimentation
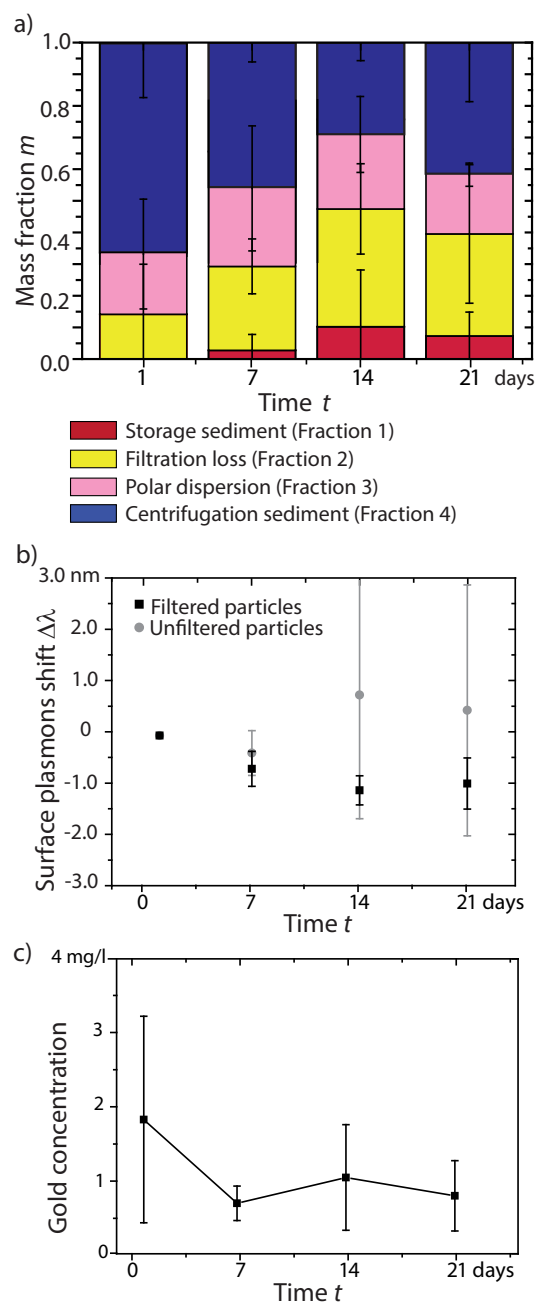
Figure 5: Fractionation (a) under inert storage. The different fraction stays constant upon storage which implies that argon prevent oxidation. Surface plasmon resonance shifts (b) of filtered (black) and unfiltered samples (grey). Gold concentrations (c) in the supernatant.

and changes in polarity upon purification and ageing. Ligand loss was not effectively prevented by storage at 7 °C or as dry particles. It was exacerbated by washing and could not be reverted by adding excess ligand. Only storage in inert argon did reduce ageing. We recommend storage of thiol-stabilized AuNP in an inert gas under exclusion of water and oxygen.

From a surface chemical standpoint, it appears that reactions involving thiol, gold, oxygen and possibly water and solvent take place during ageing. The exact mechanisms are unknown; it is unclear in which form the ligands (and gold atoms) leave the particles' surface, whether the gold surface with its catalytic properties enhances the desorption reactions, and whether small traces of chlorine remain on the particles that catalyze the reaction.[10] From a colloidal standpoint, it is interesting that details of the ligand chemistry so severely affect stability and behaviour of the entire dispersion. The small number of ligand molecules on nanoparticles compared to classical colloids seems to make them more sensitive to the loss of some of them. Small changes in the particle-ligand structure strongly affect the particles' stability in different solvents.

The sensitivity of particle behaviour on the exact ligand layer structure implies a need for more advanced ligand chemistry. It should be possible to exactly define the structure of this layer — for example, by cross-linking ligand molecules or their mixtures on the surface — and to design solubility, agglomeration behaviour, and other important properties. Such ligand layers would be more stable, more reliable and could be better tailored to the application at hand.

Acknowledgement

Supporting Information Available

The Supporting Information contains details of the preparation of samples for characterization, atomic adsorption spectroscopy, analytical centrifugation, determination of mass fractions, dynamic light scattering results and transmission profiles of isopropanol-containing gold dispersions for different storage conditions and times.

This material is available free of charge via the Internet at `http://pubs.acs.org/`.

References

(1) Weisbecker, C. S.; Merritt, M. V.; Whitesides, G. M. *Langmuir* **1996**, *12*, 3763–3772.

(2) Lin, S.-Y.; Tsai, Y.-T.; Chen, C.-C.; Lin, C.-M.; Chen, C.-h. *The Journal of Physical Chemistry B* **2004**, *108*, 2134–2139.

(3) Love, J. C.; Estroff, L. A.; Kriebel, J. K.; Nuzzo, R. G.; Whitesides, G. M. *Chemical Reviews* **2005**, *105*, 1103–1170.

(4) Dollefeld, H.; Hoppe, K.; Kolny, J.; Schilling, K.; Weller, H.; Eychmuller, A. *Phys. Chem. Chem. Phys.* **2002**, *4*, 4747–4753.

(5) Kalyuzhny, G.; Murray, R. W. *The Journal of Physical Chemistry B* **2005**, *109*, 7012–7021.

(6) Aldana, J.; Wang, Y. A.; Peng, X. *Journal of the American Chemical Society* **2001**, *123*, 8844–8850.

(7) Cheng, G.; Dennis, C. L.; Shull, R. D.; Walker, A. R. H. *Crystal Growth & Design* **2009**, *9*, 3714–3720.

(8) Hostetler, M. J.; Templeton, A. C.; Murray, R. W. *Langmuir* **1999**, *15*, 3782–3789.

(9) Djebaili, T.; Richardi, J.; Abel, S.; Marchi, M. *The Journal of Physical Chemistry C* **2013**, *117*, 17791–17800.

(10) Dasog, M.; Scott, R. W. J. *Langmuir* **2007**, *23*, 3381–3387.

(11) Chechik, V. *Journal of the American Chemical Society* **2004**, *126*, 7780–7781.

(12) Ma, Y.; Chechik, V. *Langmuir* **2011**, *27*, 14432–14437.

(13) Hak, S.; Helgesen, E.; Hektoen, H. H.; Huuse, E. M.; Jarzyna, P. A.; Mulder, W. J.; Haraldseth, O.; Davies, C. d. L. *ACS Nano* **2012**, *6*, 5648–5658.

(14) Georgiev, G. A.; Sarker, D. K.; Al-Hanbali, O.; Georgiev, G. D.; Lalchev, Z. *Colloids and Surfaces B: Biointerfaces* **2007**, *59*, 184 – 193.

(15) Wang, Y. F.; Yang, R. Q.; Shi, Z. X.; Liu, J. J.; Zhao, K.; Wang, Y. J. *Journal of Saudi Chemical Society* **2014**, *18*, 13 – 18.

(16) Loza, K.; Diendorf, J.; Sengstock, C.; Ruiz-Gonzalez, L.; Gonzalez-Calbet, J. M.; Vallet-Regi, M.; Koller, M.; Epple, M. *J. Mater. Chem. B* **2014**, *2*, 1634–1643.

(17) Woehrle, G. H.; Brown, L. O.; Hutchison, J. E. *Journal of the American Chemical Society* **2005**, *127*, 2172–2183.

(18) Kanninen, P.; Johans, C.; Merta, J.; Kontturi, K. *Journal of Colloid and Interface Science* **2008**, *318*, 88 – 95.

(19) Piot, L.; Le Floch, S.; Cornier, T.; Daniele, S.; Machon, D. *The Journal of Physical Chemistry C* **2013**, *117*, 11133–11140.

(20) Zheng, N.; Fan, J.; Stucky, G. D. *JACS* **2006**, *128*, 6550–6551.

(21) Sweeney, S. F.; Woehrle, G. H.; Hutchison, J. E. *Journal of the American Chemical Society* **2006**, *128*, 3190–3197.

(22) Balasubramanian, S. K.; Yang, L.; Yung, L. L.; Ong, C.-N.; Ong, W.-Y.; Yu, L. E. *Biomaterials* **2010**, *31*, 9023 – 9030.

(23) Ferreira, M. F.; Mousavi, B.; Ferreira, P. M.; Martins, C. I. O.; Helm, L.; Martins, J. A.; Geraldes, C. F. G. C. *Dalton Trans.* **2012**, *41*, 5472–5475.

(24) Kersey, F. R.; Merkel, T.; Perry, J. L.; Napier, M. E.; DeSimone, J. M. *Langmuir* **2012**, *28*, 8773–8781.

(25) Goertz, V.; Weis, F.; Keln, E.; Nirschl, H.; Seipenbusch, M. *Aerosol Science and Technology* **2011**, *45*, 1287–1293.

(26) Born, P.; Kraus, T. *Phys Rev E* **2013**, *6*, 062313.

(27) Mulvaney, P. *Langmuir* **1996**, *12*, 788–800.

(28) Mulvaney, P.; Perez-Juste, J.; Giersig, M.; Liz-Marzan, L.; Pecharroman, C. *Plasmonics* **2006**, *1*, 61–66.

(29) Jain, P. K.; Qian, W.; El-Sayed, M. A. *Journal of the American Chemical Society* **2006**, *128*, 2426–2433.

(30) Garnett, J. C. M. *Philosophical Transactions of the Royal Society of London. Series A, Containing Papers of a Mathematical or Physical Character* **1904**, *203*, 385–420.

(31) Moores, A.; Goettmann, F. *New J. Chem.* **2006**, *30*, 1121–1132.

(32) Maier, S. A.; Brongersma, M. L.; Kik, P. G.; Meltzer, S.; Requicha, A. A. G.; Atwater, H. A. *Advanced Materials* **2001**, *13*, 1501–1505.

(33) Hutter, E.; Fendler, J. H. *Advanced Materials* **2004**, *16*, 1685–1706.

(34) Ben, X.; Park, H. S. *J. Phys. Chem. C* **2011**, *115*, 15915–15926.

(35) Jain, P. K.; El-Sayed, M. A. *J. Phys. Chem. C* **2008**, *112*, 4954–4960.

(36) Benfield, R.; Creighton, J.; Eadon, D.; Schmid, G. *Zeitschrift für Physik D Atoms, Molecules and Clusters* **1989**, *12*, 533–536.

(37) Joseph, Y.; Guse, B.; Nelles, G. *Chemistry of Materials* **2009**, *21*, 1670–1676.

Graphical TOC Entry